

Nonketotic hyperglycinemia: spectrum of imaging findings with emphasis on diffusion-weighted imaging

Shaimaa Abdelsattar Mohammad¹ · Heba Salah Abdelkhalek²

Received: 29 May 2017 / Accepted: 22 August 2017 / Published online: 1 September 2017
© Springer-Verlag GmbH Germany 2017

Abstract

Purpose The purpose of this study was to explore brain abnormalities in nonketotic hyperglycinemia (NKH) using diffusion-weighted imaging (DWI) and when feasible, diffusion tensor imaging (DTI) and tractography.

Methods Seven patients with confirmed diagnosis of NKH (8 days–2 years) underwent brain MRI. Conventional T1 and T2WI were acquired in all patients, DWI in six and DTI and tractography in two (4 months and 2 years). Measurements of fractional anisotropy (FA), radial diffusivity (RD), axial diffusivity (AD) and Trace from eight white matter regions were compared between the two patients and age-matched controls. Tractography of corpus callosum, superior longitudinal fasciculus and corticospinal tracts was performed with extraction of their FA and diffusivity indices.

Results MRI showed nonspecific brain atrophy in three children. Corpus callosum atrophy was found as a part of these atrophic changes. Cerebellar vermian hypoplasia and supratentorial hydrocephalus were seen in one patient. The topographic distribution of diffusion restriction was different

among patients. The affected white matter regions were not predominantly following the expected areas of myelination according to patients' age. Deep grey matter nuclei were affected in one patient. DTI revealed lower FA with higher RD in most of the measured white matter regions and tracts. These changes were more appreciated in the 2-year-old patient. However, Trace was higher in the 2-year-old patient and lower in the 4-month-old one. The extracted tracts were decreased in volume.

Conclusion DWI, DTI and tractography with FA and diffusivity measurements can give insights into white matter microstructural alterations that can occur in NKH.

Keywords Vacuolating myelinopathy · Diffusion-weighted image (DWI) · Diffusion tensor imaging (DTI) · Fractional anisotropy · Corpus callosum

Introduction

Nonketotic hyperglycinemia (NKH) is a rare neurometabolic disease with an autosomal recessive inheritance. It results from a defect of glycine cleavage system resulting in accumulation of the neurotoxic glycine in the brain and body fluids. Neonatal form is the most common clinical phenotype. It manifests with encephalopathy and breathing difficulties with multifocal myoclonic seizures. Death mostly occurs in the first year of life, and those who survive display severe neurodevelopmental delay with intractable seizures [1].

Neuroimaging features of NKH in neonatal period are previously described in a few reports focusing on abnormal white matter signal in dorsal pons and midbrain and posterior limb of internal capsule with extreme thinning of the corpus callosum [2–4]. Identification of abnormalities in the early phase of injuries is important for early diagnosis and for

Electronic supplementary material The online version of this article (<https://doi.org/10.1007/s00234-017-1913-0>) contains supplementary material, which is available to authorized users.

✉ Shaimaa Abdelsattar Mohammad
Shaimaa96@hotmail.com

Heba Salah Abdelkhalek
hsalahabd@yahoo.com

¹ Radiodiagnosis Department, Faculty of Medicine, Ain-Shams University, 9 Lotfi Elsayed St. Ain-Shams University Staff Buildings, Cairo 11657, Egypt

² Medical Genetics Unit, Pediatric Department, Faculty of Medicine, Ain-Shams University, Cairo, Egypt

understanding the pathogenesis. Routinely used neonatal ultrasound and conventional MR pulse sequences could have poor sensitivity to significant abnormalities in neonatal brains. However, diffusion-weighted MR imaging provides information that is not apparent on conventional sequences. White matter abnormalities are related to myelin vacuolation that results in diffusion restriction in the affected regions [4].

To our knowledge, few reports in the literature describing white matter abnormalities on diffusion-weighted images in NKH exist [4–10]. Moreover, to the best of our knowledge, only two reports documenting the diffusion tensor imaging findings in NKH [9, 11] without any data about the white matter tracts or measurements of anisotropy and diffusivity indices that can reflect white matter microstructural alterations. The aim of this study was to explore brain abnormalities and white matter alterations that can occur in nonketotic hyperglycinemia (NKH) using diffusion-weighted imaging (DWI), and when feasible, diffusion tensor imaging (DTI) and tractography.

Material and methods

Patients

After ethical committee approval, a cross-sectional study was conducted on children with NKH (diagnosed at medical genetics unit Ain-Shams University) from Jan 2015 to Jan 2016. Eight children were initially included. One of them died before MRI imaging; therefore, seven children were enrolled (three girls and four boys). Their age range is 8 days to 2 years. The diagnosis was confirmed with elevated CSF glycine and CSF/serum glycine ratio. To avoid misdiagnosis of ketotic hyperglycinemia, organic acid urine analysis was performed and it was unremarkable. Enzymatic assay on liver biopsy was not performed. Six patients underwent MRI at our hospital; the last patient was referred after having MRI performed at another institute.

MRI examination

All patients were scanned with a 1.5-T scanner (Achieva, Philips Healthcare, Best, The Netherlands) using eight-channel SENSE head coil (SENSE acceleration factor of 8). The following MRI sequences were included in the MRI brain protocol used in our department: axial and sagittal T1WI (TR/TE: 542/15), axial fast spin-echo double echo sequence (neonate to 3 months TR/TE: 3000/40,120; 3–6 months 3000/30,100; > 6 months 2500/30,100 ms) and T1-WIR (TR/TE/TI: 2000/15/750 ms). Diffusion-weighted images were performed in six patients as the last patient who was referred after MRI had been performed at another institute. Single-shot spin-echo echo-planar imaging (TR/TE

3000/100) was with diffusion sensitivities b_0 and 1000 s/mm^2 . Three sets of axial DWI were generated following the application of diffusion gradients in three orthogonal planes. A composite isotropic Trace image and apparent diffusion coefficient map (ADC) were then made and used for analysis.

Owing to the prolonged imaging time and unavailability of control subjects in this very young age, DTI was performed only in the first two children enrolled in the study, along with two age-matched control subjects complaining of fits with no evidence of structural brain aberrations or signal intensity abnormality on conventional and diffusion-weighted images. The DTI data were acquired using single shot echo-planar sequence. In addition to baseline b_0 image, diffusion-weighted images were acquired in 16 noncollinear direction. Sixty axial slices with 2 mm slice thickness were positioned parallel to the anterior-posterior commissure line. The field of view was 224 mm \times 224 mm and in-plane resolution = 1.75 \times 1.75 mm^2 .

MRI analysis

Brain MRI examinations were analyzed for any structural abnormalities. Myelination was assessed by revising the white matter signal intensity on T1 and T2WI. Pattern of insufficient myelination was documented if there was lack of the myelin signal intensity on T1WI and T2WI in structures that are expected to be myelinated according to the patients' age.

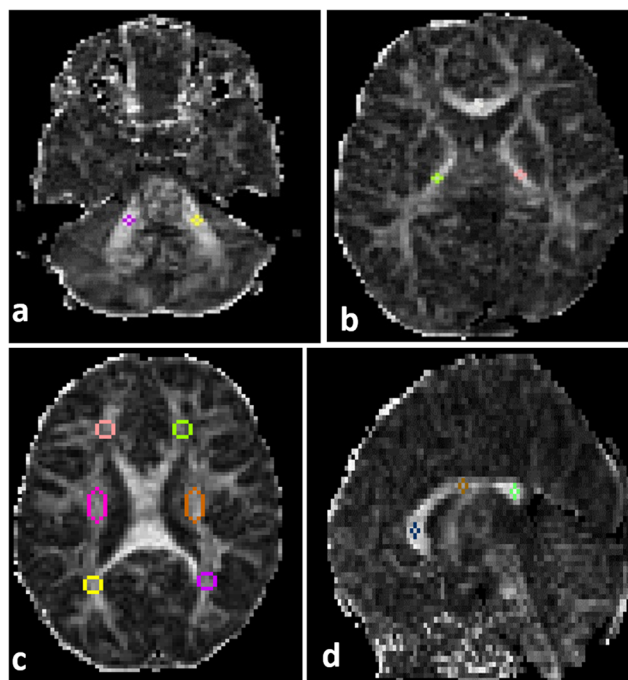


Fig. 1 Regions of interest displayed on fractional anisotropy map. **a** Middle cerebellar peduncles. **b** Posterior limb of internal capsule. **c** Frontal white matter, corona radiata and parietal white matter from anterior to posterior. **d** Genu, body and splenium of corpus callosum (from anterior to posterior)

Table 1 Spectrum of the imaging findings

	Gender	Age at MRI	Grey matter abnormality	White matter abnormality on T1 and T2WI	Diffusion restriction	Other findings
<i>1^a</i>	m	2 years	Caudate, thalamus, lentiform atrophy without abnormal signal	No abnormal signal	Negative	Ventricular dilatation ex-vacuo
<i>2^a</i>	f	8 days	None	PLIC	SCP, PLIC, centrum semiovale	None
<i>3^a</i>	m	8 days	None	CTT and PLIC	Pyramidal tracts in pons, ICP, MCP, SCP, CTT, cerebellar white matter, PLIC, CR	None
<i>4^a</i>	m	4 months	Caudate, lentiform atrophy without abnormal signal	MCP, PLIC, centrum semiovale	Pyramidal tracts in pons, CTT, MCP, ALIC, PLIC, periventricular white matter, centrum semiovale	Vermian hypoplasia, communicating hydrocephalus
<i>5^a</i>	m	5 months	None	ALIC, PLIC	MCP, transverse pontine fibres, ALIC, PLIC, CC, diffuse cerebral white matter signal abnormality	Ventricular dilatation ex-vacuo
<i>6^a</i>	f	7 months	Dentate, thalamus, globus pallidus, red nucleus and substantia nigra as part of diffuse cerebral peduncle involvement	CTT, ICP, cerebral peduncles	Dentate, thalamus, globus pallidus CTT, ICP, red nucleus and substantia nigra as part of diffuse cerebral peduncle involvement	Ventricular dilatation ex-vacuo
<i>7</i>	f	6 months	Globus pallidus	PLIC, splenium of corpus callosum	Not performed	None

Italicized entries indicate patients who underwent DTI

ALIC anterior limb of internal capsule, CC corpus callosum, CR corona radiata, CTT central tegmental tract, f female, ICP inferior cerebellar peduncles, m male, MCP middle cerebellar peduncles, PLIC posterior limb of internal capsule, SCP superior cerebellar peduncles

^a MRI scans were performed at our institution

Diffusion restriction was documented if the bright signal on Trace DWI was accompanied by low signal on ADC map.

DTI data set was analyzed by using DTI Studio software produced by this laboratory (H. Jiang and S. Mori, Johns Hopkins University and Kennedy Krieger institute, <http://godzilla.kennedykrieger.org> or <http://lbam.med.jhmi.edu>) [12]. The raw diffusion-weighted images were co-registered to b0 images and then corrected for small subject motion using automatic image registration. FA and its colour map, radial diffusivity (RD), axial diffusivity (AD) and Trace were calculated in the native space.

Tractography of three major white matter tracts was then performed according to Fibre Assignment by Continuous Tracking (FACT) method [13] described by Wakana et al. (corpus callosum as a largest commissural tract, corticospinal tract as a projection tract and superior longitudinal fasciculus as an association tract). FA, RD, AD and Trace were calculated for each tract on both hemispheres and then averaged.

We applied the region of interest (ROI) approach to study different white matter regions (corona radiata, CR; frontal white matter, FWM; parietal white matter, PWM; middle cerebellar peduncles, MCP; posterior limb of internal capsule,

PLIC; genu, body and splenium of corpus callosum). ROIs are manually drawn on brain images in the native space by using ROI Editor Software (Li X, Jiang H, and Mori S: Johns Hopkins University; [www. MriStudio.org](http://www.MriStudio.org)) (Fig. 1). We tried to draw ROIs of consistent size and at consistent locations between subjects. The ROIs of CR, FWM and PWM were drawn at the same axial slice at the level of the body of the corpus callosum and MCP at the level of the mid pons. Another ROI was drawn at midportion of the PLIC at the level where fornix was identified as single intense structure. Corpus callosum ROIs were evaluated in mid sagittal images in the genu, body and splenium at their midportions. The average of each ROI for both hemispheres was used for analysis with calculation of the percentage of increase or reduction of the patients' ROI values in relation to controls'.

Results

The study included seven children with confirmed diagnosis of neonatal form of NKH. Consanguineous parents were present in five patients and positive history of previous sibling death was present in four, ranging from one to four sibling deaths. The main presenting symptoms were poor suckling and lethargy that were progressed to convulsions and coma. The first symptom started at the age ranged from 1 to 14 days. CSF glycine ranged from 105 to 230.4 $\mu\text{mol/L}$ (reference range 2–40 $\mu\text{mol/L}$); CSF/serum glycine ratio ranged from 0.26 to 0.65 (reference range 0.012–0.04) at the time of diagnosis. All patients were under treatment by sodium benzoate (500 mg/kg/day). One patient died at the age of 4 months, and those who survived developed severe global developmental delay.

MRI features are summarized in Table 1. MRI showed non-specific brain atrophy in three children; corpus callosum atrophy was found as a part of these atrophic changes. Additional cerebellar vermian hypoplasia and supratentorial hydrocephalus were seen in one patient. Subtle abnormal signal on T1 WI and T2WI was seen in six patients indicating deficiency of normal myelination with white matter oedema in sites expected to have normal myelin according to the myelination time table. White matter abnormalities were better depicted on diffusion-weighted images (Fig. 2) which were available in six patients. Diffusion restriction was observed in infratentorial and supratentorial structures in five patients. Variable degrees of supratentorial white matter diffusion restriction were seen ranging from subtle centrum semiovale and corona radiata abnormality in the two 8-day-old patients (Fig. 3) to periventricular and even subcortical white matter involvement in 4- and 5-month-old patients, respectively (Fig. 4). PLIC was affected in four patients; central tegmental tracts and MCP in three; superior cerebellar peduncles and pyramidal tracts at the pons in two; and cerebral peduncles, inferior cerebellar peduncles and cerebellar

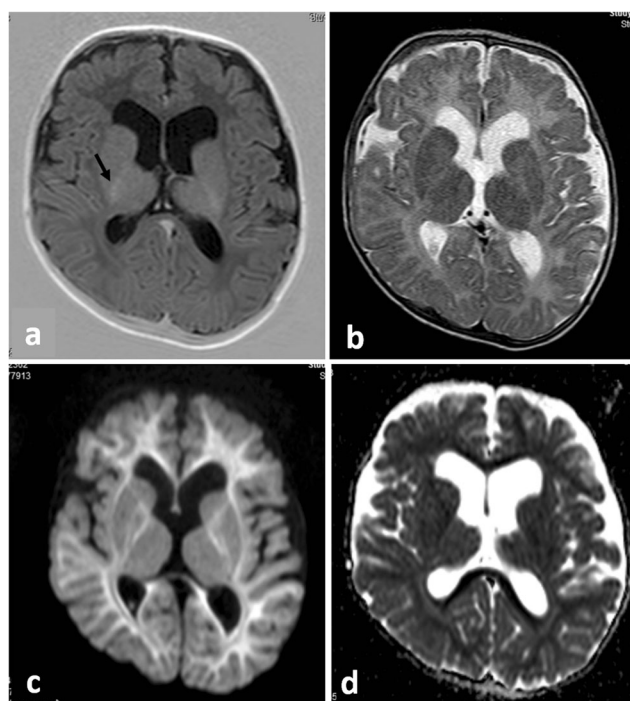
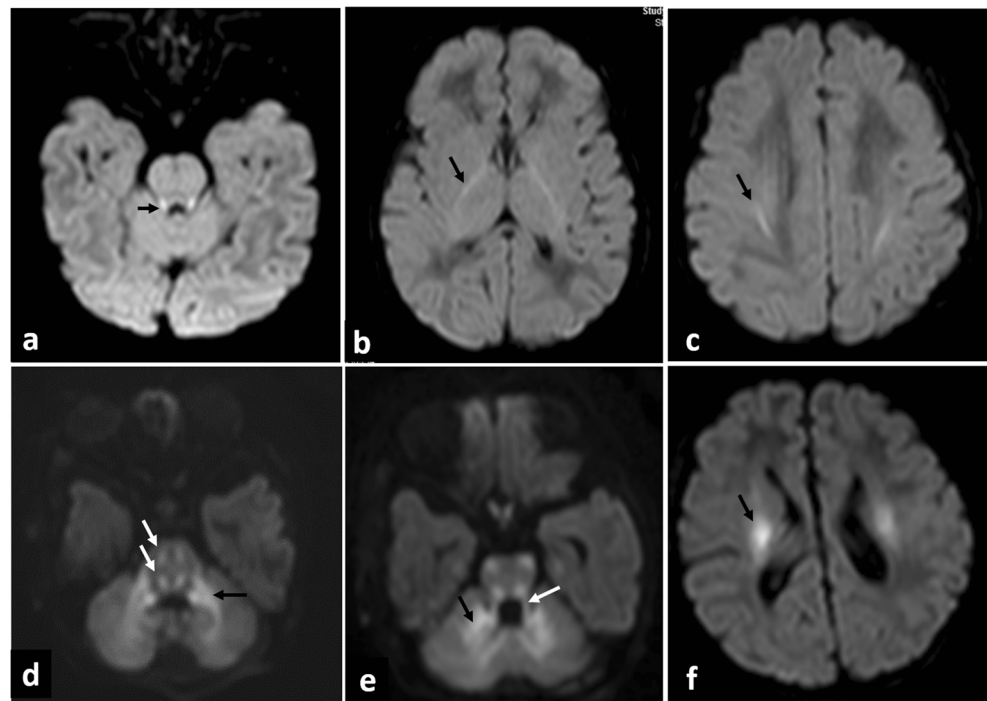


Fig. 2 MRI brain of 5-month-old boy (patient 5). **a** Axial T1 WI showing faint hyperintense signal of myelin in the posterior limb of internal capsule (arrow). **b** Axial T2WI shows limited ability of the T2WI to demonstrate the extent of white matter abnormality. **c** DWI and **d** ADC show extensive white matter diffusion restriction extending to the subcortical white matter. White matter exhibits hyperintense signal on DWI and hypointense signal on ADC

white matter in only one patient. Grey matter diffusion restriction was seen in the 7-month-old patient (patient 6) diffusely involving the thalamus, globus pallidus and dentate with involvement of the red nucleus and substantia nigra as part of diffuse cerebral peduncles abnormal signal. This was associated with involvement of the inferior cerebellar peduncles and central tegmental tracts (Fig. 5) with no hemispheric white matter involvement. Atrophy of the basal ganglia without abnormal signal was seen in the 2-year- and 4-month-old patients (patients 1 and 4).

DTI was performed in two patients (patient 1 and 4; 2 years and 4 months, respectively). Tractography of the corpus callosum, superior longitudinal fasciculus (SLF) and corticospinal tract (CST) was performed in patient 1. In patient 4, the SLF could not be traced because of his young age; the corpus callosum also could not be traced as it was markedly thinned and stretched by the effect of hydrocephalic changes. DTI revealed decreased signal intensity on FA maps with decreased colour hue on colour FA maps in the 2-year-old patient (patient 1) (Fig. 6) and to lesser degree the 4-month-old patient (patient 4) (Fig. 7), reflecting decreased white matter anisotropy. Most of the white matter regions and tracts demonstrated lower FA showing 9.2 to 57.14% reduction in the 2-year-old patient (Fig. 8) and 2.17 to 34.55% reduction in the 4-month-old patient compared to age-matched controls.

Fig. 3 Sequential axial DWI demonstrating different distributions of diffusion restriction in two different patients 8 days old. Upper row (patient 2) demonstrates diffusion restriction in the superior cerebellar peduncles (arrow, **a**), posterior limb of internal capsule (arrow, **b**) and centrum semiovale (arrow, **c**). Lower row (patient 3) demonstrates diffusion restriction in the dorsal and ventral brain stem tracts (white arrows, **d**), middle cerebellar peduncles (black arrow, **d**), superior cerebellar peduncles (white arrow, **e**), cerebellar white matter (black arrow, **e**) and corona radiata (arrow, **f**)



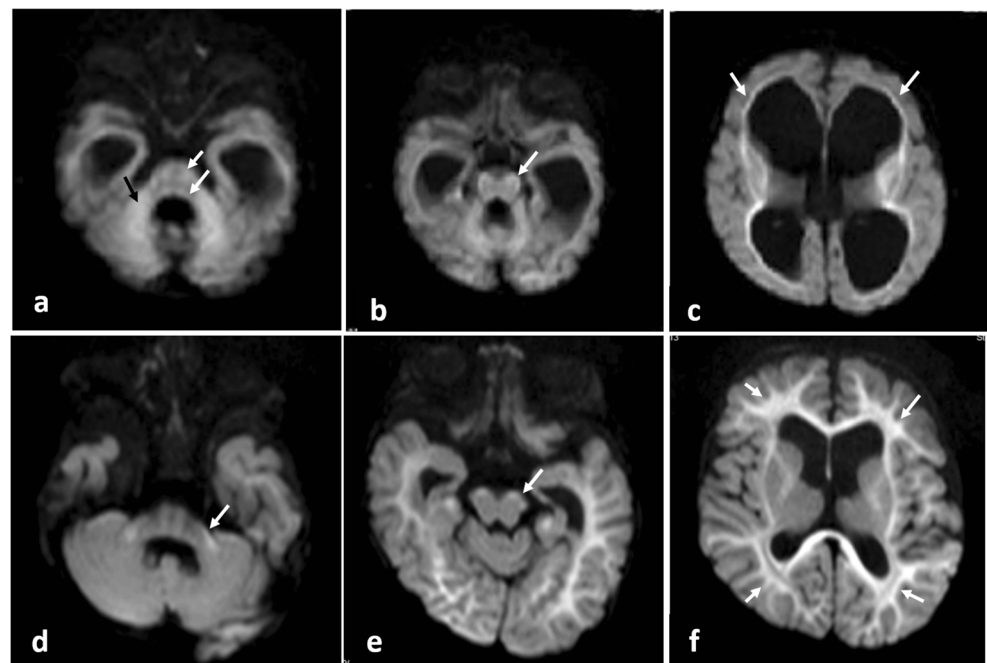
On the contrary, RD was higher in the two patients. It showed 8.15 to 147% increase in the 2-year-old patient (Fig. 8) and 0.74 to 2.9% increase in the 4-month-old patient. On the other hand, most of the white matter regions in the 2-year-old patient demonstrated higher Trace values (0.79 to 47.53% increase), while the 4-month-old patient (patient 4) demonstrated lower Trace values (0.69 to 38.3% reduction). Minimal changes of AD were detected in both patients (supplementary Tables e-1 and e-2). In addition to the measured anisotropy

and diffusivity indices, we found that extracted tracts showed decrease in their volume (Fig. 9).

Discussion

Metabolic disorders are considered one of the important causes of encephalopathy in the neonatal period [14, 15]. MRI can provide diagnostic information that is crucial for

Fig. 4 Sequential axial DWI demonstrating different distributions of diffusion restriction in two different patients 4 and 5 months old. Upper row (patient 4) demonstrates faint diffusion restriction in the middle cerebellar peduncles (black arrow, **a**) and dorsal and ventral brain stem tracts (white arrows, **a**) with dark signal on ADC (not shown), cerebral peduncles (arrow, **b**) and periventricular white matter (arrows, **c**). Lower row (patient 5) demonstrates diffusion restriction in the middle cerebellar peduncles (arrow, **d**), cerebral peduncles (arrow, **e**) and hemispheric white matter extending to the subcortical regions (arrows, **f**)



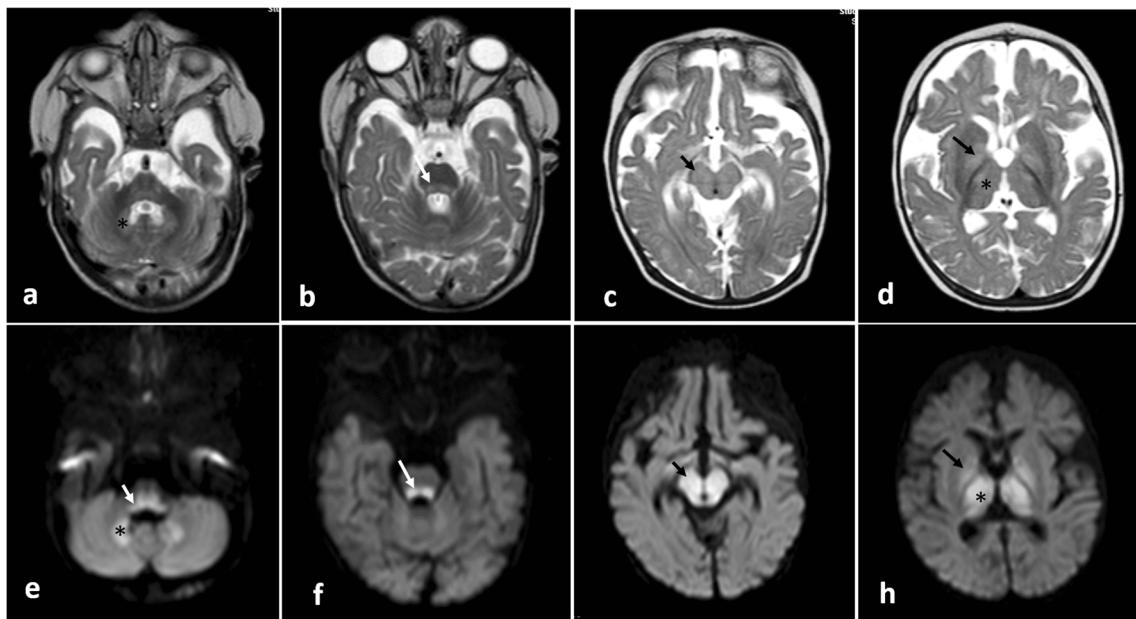


Fig. 5 Axial T2WI (upper row) and DWI (lower row) of 7-month-old girl (patient 6). The dentate (asterisk, **a, e**) and inferior cerebellar peduncle (arrow, **e**) exhibit abnormal signal as well as central tegmental tracts

(arrows, **b, f**); the whole midbrain including cerebral peduncles (arrow, **c, g**) signifying substantia nigra and red nucleus affection; globus pallidus (arrow, **d, h**) and thalamus (asterisk, **d, h**)

Fig. 6 Axial T2WI (**a, b**), axial T1WI (**c**), colour FA map (**d, e**), FA map (**f**) of 2-year-old boy with NKH and colour map and FA map of age-matched control (**g–i**), demonstrating nonspecific brain atrophy with no abnormal signal on conventional T1 and T2WI. However, there is decreased colour hue (**d, e**) and anisotropy (**f**) compared to the control subject

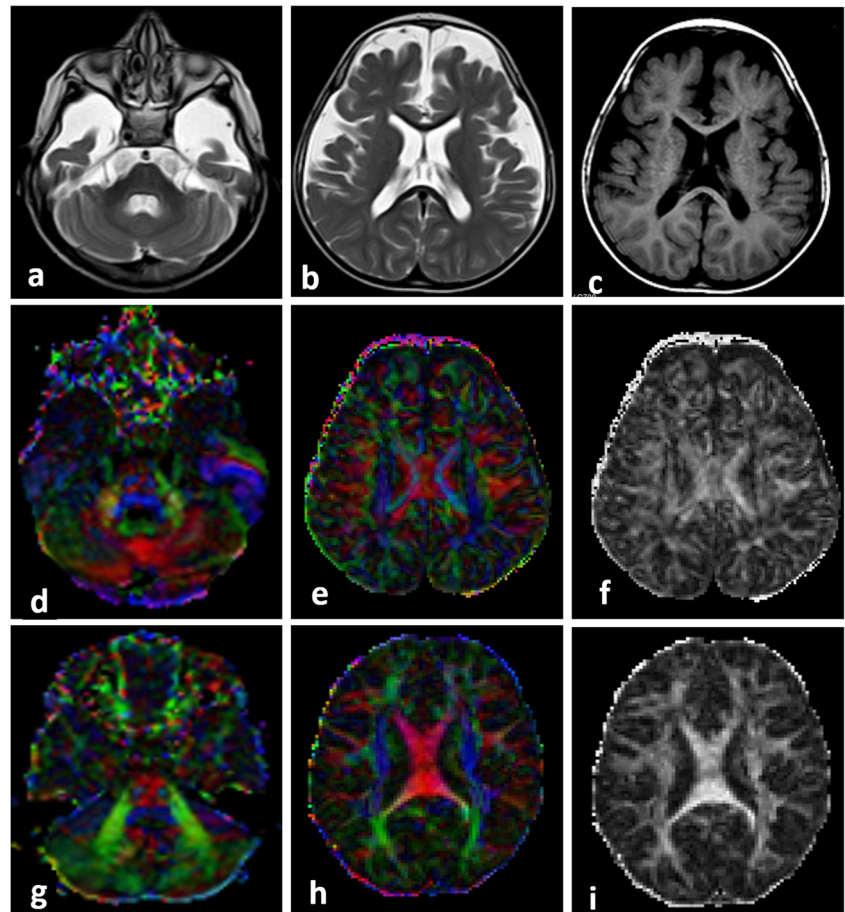
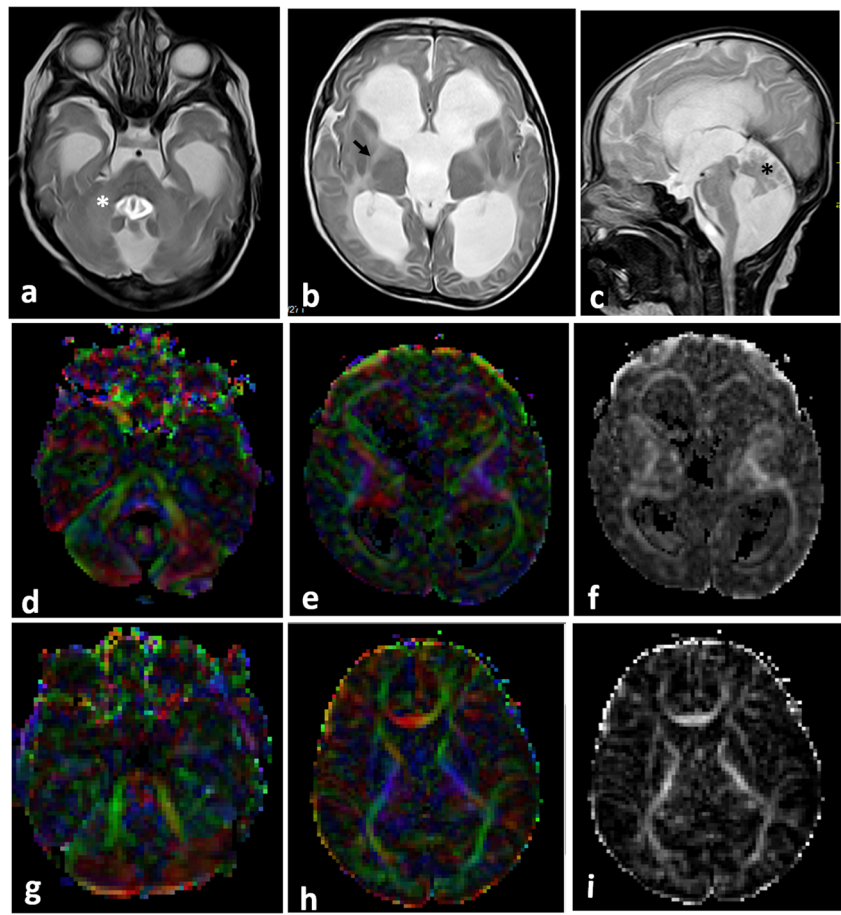


Fig. 7 Axial T2WI (a, b), sagittal T2WI (c), colour FA map (d, e), FA map (f) of 4-month-old boy with NKH and colour map and FA map of age-matched control (g–i), demonstrating abnormal T2 signal is seen in the middle cerebellar peduncles (white asterisk), posterior limb of internal capsule (arrow) associated with hydrocephalic changes, vermian hypoplasia (black asterisk). There is decreased colour hue (d, e) and anisotropy (f) compared to the control subject



differential diagnosis and, consequently, optimal treatment strategy. It is well known that diffusion-weighted images can depict abnormalities earlier than conventional sequences especially in neonates and young infants whose brain normally has higher water content (predominantly high signal on T2WI and low signal on T1WI) [14]. MRI features of NKH have been described in a few case reports mostly presenting patients in neonatal period [3–5]. In our series, we described MRI findings of patients in neonatal period and early infancy focusing on brain diffusion characteristics.

NKH is one of the metabolic diseases that induce vacuolating myelinopathy [14, 15]. Due to the young age of most of our patients (below 1 year of age), conventional MR sequences (T1 and T2WI) had limited ability to properly define the extent of white matter abnormality [2]. Although it was reported that the abnormal signal on T2WI and DWI was confined to white matter regions that were normally expected to be myelinated at a given age (the dorsal brain stem, PLIC and corona radiata) [4–6, 10, 11, 15], we have found diffusion restriction in other regions not necessarily following expected

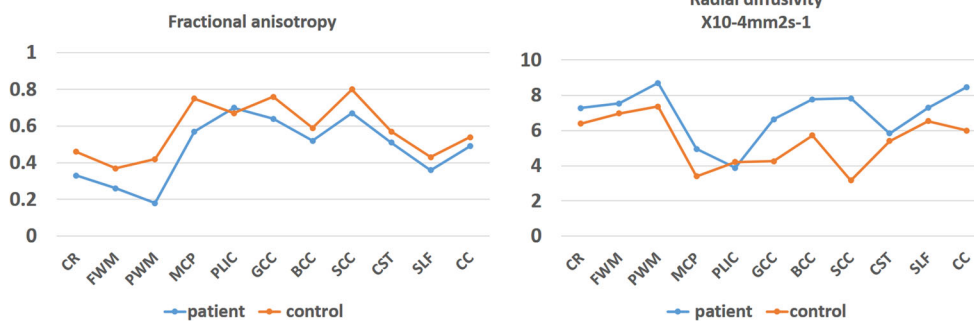
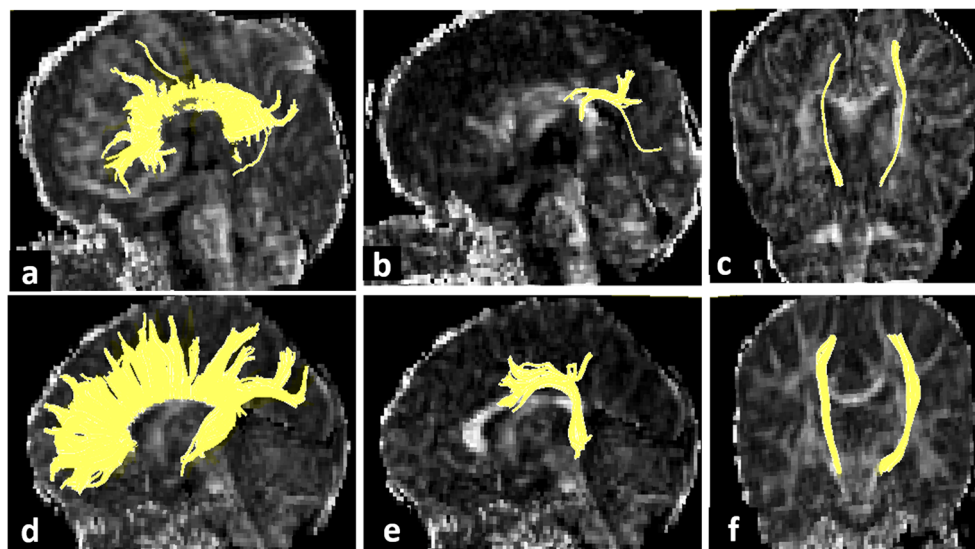


Fig. 8 Fractional anisotropy and radial diffusivity values for various white matter regions of 2-year-old boy with NKH and age-matched control. CR, corona radiata; FWM, frontal white matter; PWM, parietal white matter; MCP, middle cerebellar peduncle; PLIC, posterior limb of

internal capsule; GCC, Genu of the corpus callosum; BCC, body of the corpus callosum; SCC, splenium of the corpus callosum; CST, corticospinal tract; SLF, superior longitudinal fasciculus; CC, corpus callosum

Fig. 9 Tractography of the 2-year-old patient (a–c) and age-matched control (d–f). The reconstructed tracts appear to be reduced in size in the patient compared to control subject. **a, d** Corpus callosum. **b, e** Superior longitudinal fasciculus. **c, f** Corticospinal tract



areas of myelination. The two neonates (8 days) in this study had different distributions of diffusion restriction despite similar clinical condition and laboratory profile. We have found diffusion restriction not only in the dorsal brainstem tracts but also ventrally in agreement with few case reports that illustrated diffusion restriction in the ventral tracts of the brain stem [4, 7]. Moreover, the diffusion restriction was seen extending to the subcortical white matter in the 5-month-old boy, the region which was not expected to be myelinated at this age. In addition, the 7-month-old girl had limited white matter diffusion restriction confined to infratentorial locations with no supratentorial white matter involvement. It was documented that diffusion restriction in the cerebral white matter disappears at 17-months of age [11]. Disappearance of white matter diffusion restriction was explained by coalescence of myelin vacuoles with advanced age [3]. We could suggest that this process could occur earlier than previously speculated.

DTI can give new insights of white matter microstructural alterations that can occur secondary to inherited white matter diseases [10, 16]. FA (the index of the amount of anisotropy) is the quantitative biomarker of white matter integrity. FA can be related to several histological characteristics, such as axonal density and diameter, as well as degree of myelination, and the increase of FA is related to the increase in the connectivity of white matter bundles. It was documented that FA in NKH patients was preserved at the neonatal period and at the age of 3 months and decreased by the age of 17 months [9, 11]. We have found that anisotropy was diminished on FA map with decreased colour hue on colour map in the 2-year-old patient and to a lesser extent in the 4-month-old patient compared to controls. RD expresses diffusivity perpendicular to the direction of fibre orientation. RD and Trace measurements reflect myelin changes [17, 18]. We found that the higher RD in patients compared to controls was more appreciated in the older patient (2 years old). These observed changes in FA,

RD and Trace could reflect more myelin deficiency with progressive decrease in white matter integrity with advancing age. On the contrary, Trace was lower in the 4-month-old boy than the control reflecting diffusion restriction within the myelin vacuoles early in the disease process. In addition, we have found minimal AD changes in the two patients indicating limited axonal changes compared to the obvious changes in myelin. This indicates that the main changes in anisotropy are related to myelin rather than axonal changes. Interestingly, in spite of the obvious changes at FA and colour map in the 2-year-old patient (patient 1), no detectable signal abnormality was seen on T2WI or DWI, emphasizing the role of DTI in detection of white matter alterations. To our knowledge, the findings of changes of diffusivity indices in NKH have not been described previously.

Basal ganglia abnormality was documented in a few case reports focusing on globus pallidus [4] and dentate nucleus abnormal signal on DWI [9, 10]. Diffusion restriction in the lateral thalami was also documented in neonatal period [4, 5]. To the extent of our knowledge, our findings of diffusion restriction and T2 abnormalities diffusely involving the thalamus with involvement of red nucleus and substantia nigra (as part of diffuse cerebral peduncles abnormality) at the age of 7 month have not been previously described. Moreover, atrophy of the basal ganglia without abnormal signal which was seen in the 4-month- and 2-year-old patients as a part of whole brain atrophic changes has not been previously documented.

The glycine cleavage system is crucial for the developing neuroepithelium. With increased glycine levels, the action of glycine on glycine and *N*-methyl-D-aspartate receptors could be excitotoxic leading to deleterious effects [19, 20]. Gyral abnormalities, cerebellar vermian hypoplasia and hydrocephalus have been previously published in association with NKH [21–23]. The only child in our series with hydrocephalus died at the age of 4 months, and this agrees

with previous studies that documented poorer outcome with the presence of hydrocephalus [1]. Corpus callosum hypoplasia has been described as one of the neuroimaging findings of NKH [4]. We found that corpus callosum atrophy was seen only in patients who developed brain atrophy, and by using tractography, we found that not only the corpus callosum but also the SLF and CST were reduced in size. The decrease in the volume of the extracted tracts reflects the decrease in white matter volume that was visualized in conventional images. Consequently, the corpus callosum abnormality could represent part of the decrease in global white matter volume rather than an isolated finding.

The study was limited by relatively small number of patients of this quite rare neurometabolic disease. This was also a cross-sectional study examining MRI of patients of different ages. Longitudinal study with more number of patients will give more detailed comprehension of sequence of white matter aberrations that could occur with advancing age.

To summarize, the topographic distribution of diffusion restriction was different among patients with NKH, which was not exclusively confined to sites of expected myelination at a given age. In addition, basal ganglia including globus pallidus, the thalamus, substantia nigra, red nucleus and dentate can be affected. The FA, RD and Trace changes visualized in patients with NKH reflect myelin abnormalities observed in those patients.

Funding No funding was received for this study.

Compliance with ethical standards

Conflict of interest The authors declare that they have no conflict of interest.

Ethical approval All procedures performed in the studies involving human participants were in accordance with the ethical standards of the institutional and/or national research committee and with the 1964 Helsinki Declaration and its later amendments or comparable ethical standards.

Informed consent Informed consent was obtained from all individual participants included in the study.

References

1. Hoover-Fong JE, Shah S, Van Hove JLK (2004) Natural history of nonketotic hyperglycinemia in 65 patients. *Neurology* 63:1847–1853
2. Press GA, Barshop BA, Haas RH et al (1989) Abnormalities of the brain in nonketotic hyperglycinemia: MR manifestations. *Am J Neuroradiol* 10:315–321
3. Shah DK, Tingay DG, Fink AM et al (2005) Magnetic resonance imaging in neonatal nonketotic hyperglycinemia. *Pediatr Neurol* 33:50–52
4. Khong PL, Lam BCC, Chung BHY (2003) Diffusion-weighted MR imaging in neonatal nonketotic hyperglycinemia. *Am J Neuroradiol* 24:1181–1183
5. Kanekar S, Byler D (2013) Characteristic MRI findings in neonatal nonketotic hyperglycinemia due to sequence changes in GLDC gene encoding the enzyme glycine decarboxylase. *Metab Brain Dis* 28:717–720
6. Nicolasjilwan M, Ozer H, Wintermark M et al (2011) Neonatal nonketotic hyperglycinemia. *J Neuroradiol* 38:246–250
7. Butler CJ, Likeman M, Mallick AA (2017) Distinctive magnetic resonance imaging findings in neonatal nonketotic hyperglycinemia. *Pediatr Neurol* 72:90–91
8. Zubarioglu T, Kiykim E, Cansever MS et al (2016) Neonatal nonketotic hyperglycinemia: diffusion-weighted magnetic resonance imaging and diagnostic clues. *Acta Neurol Belg* 116:671–673
9. Culjat M, Benjak V, Dasovic-Buljevic A et al (2010) Magnetic resonance findings in a neonate with nonketotic hyperglycinemia: case report. *J Comput Assist Tomogr* 34:762–765
10. Sener RN (2003) Nonketotic hyperglycinemia: diffusion magnetic resonance imaging findings. *J Comput Assist Tomogr* 27:538–540
11. Mourmans J, Majoie CBLM, Barth PG et al (2006) Sequential MR imaging changes in nonketotic hyperglycinemia. *Am J Neuroradiol* 27:208–211
12. DTI, Jiang H, van Zijl PC, Kim J et al (2006) DtiStudio: resource program for diffusion tensor computation and fiber bundle tracking. *Comput Methods Prog Biomed* 81:106–116
13. Wakana S, Caprihan A, Panzenboeck MM et al (2007) Reproducibility of quantitative tractography methods applied to cerebral white matter. *NeuroImage* 36:630–644
14. Shroff MM, Soares-Fernandes JP, Whyte H et al (2010) MR imaging for diagnostic evaluation of encephalopathy in the newborn. *Radiographics* 30:763–780
15. Patay Z (2011) MR imaging workup of inborn errors of metabolism of early postnatal onset. *Magn Reson Imaging Clin N Am* 19:733–759
16. Isaacson J, Provenzale J (2011) Diffusion tensor imaging for evaluation of the childhood brain and pediatric white matter disorders. *Neuroimaging Clin N Am* 21:179–189
17. Song SK, Sun SW, Ramsbottom MJ et al (2002) Dysmyelination revealed through MRI as increased radial (but unchanged axial) diffusion of water. *NeuroImage* 17:1429–1436
18. Mori S, Zhang J (2006) Principles of diffusion tensor imaging and its applications to basic neuroscience research. *Neuron* 51:527–539
19. Gabis L, Parton P, Roche P (2001) In vivo ¹H magnetic resonance spectroscopic measurement of brain glycine levels in nonketotic hyperglycinemia. *J Neuroimaging* 11:209–211
20. Viola A, Chabrol B, Nicoli F (2002) Magnetic resonance spectroscopy study of glycine pathways in nonketotic hyperglycinemia. *Pediatr Res* 52:292–300
21. Dobyns WB (1989) Agenesis of the corpus callosum and gyral malformations are frequent manifestations of nonketotic hyperglycinemia. *Neurology* 39:817–820
22. Bekiesińska-Figatowska M, Rokicki D, Walecki J (2001) MRI in nonketotic hyperglycinaemia: case report. *Neuroradiology* 43:792–793
23. Manel L, Houneida ZBA et al (2012) A rare inborn error of metabolism associated with a Dandy–Walker malformation. *Acta Neurol Belg* 112:425–426